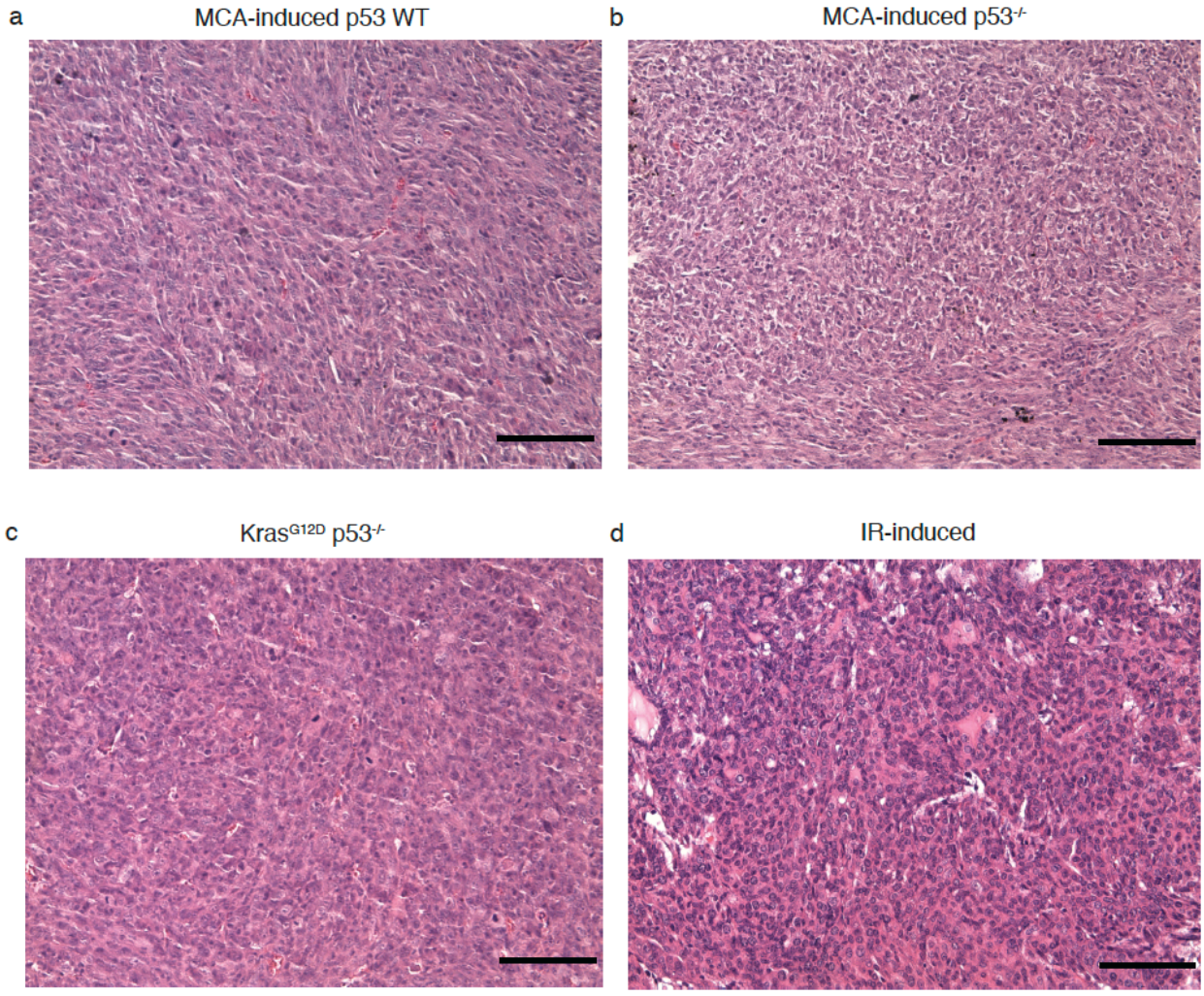

Figure S1. Representative hematoxylin and eosin (H&E) stained sections of murine soft-tissue sarcomas. **a,** MCA-induced p53 WT. **b,** MCA-induced $p53^{-/-}$. **c,** $Kras^{G12D}$; $p53^{-/-}$. **d,** IR-induced p53 WT. Scale bar, 100 μm.

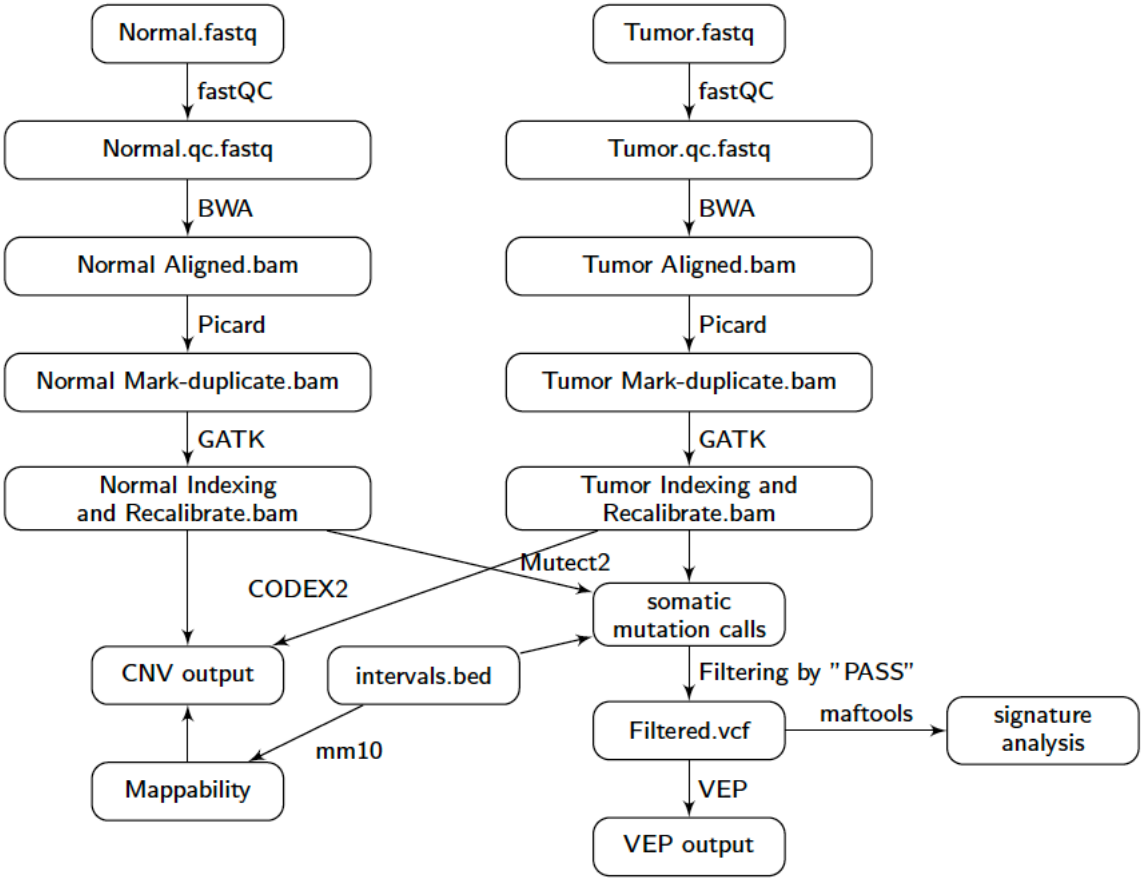

Figure S2. Schematics of the methods for processing and analyzing whole exome sequencing data from tumors and paired normal tissues.

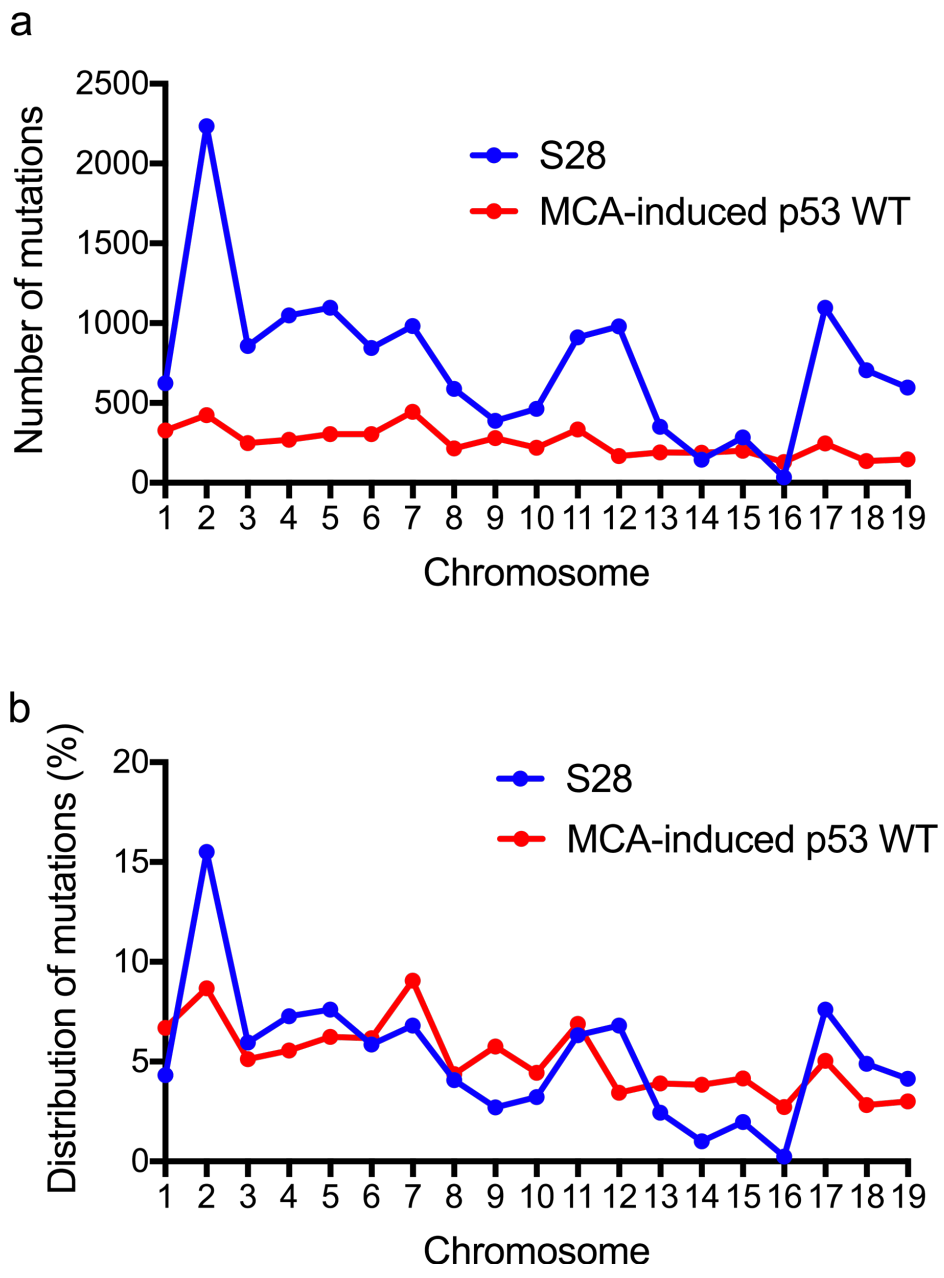

Figure S3. Comparison of mutations per chromosome between an IR-induced sarcoma (S28) and MCA-induced p53 WT sarcomas. **a,b,** The number of total somatic mutations and the distribution of total somatic mutations on each chromosome. The data of MCA-induced p53 WT sarcomas represent the average of 7 tumors.

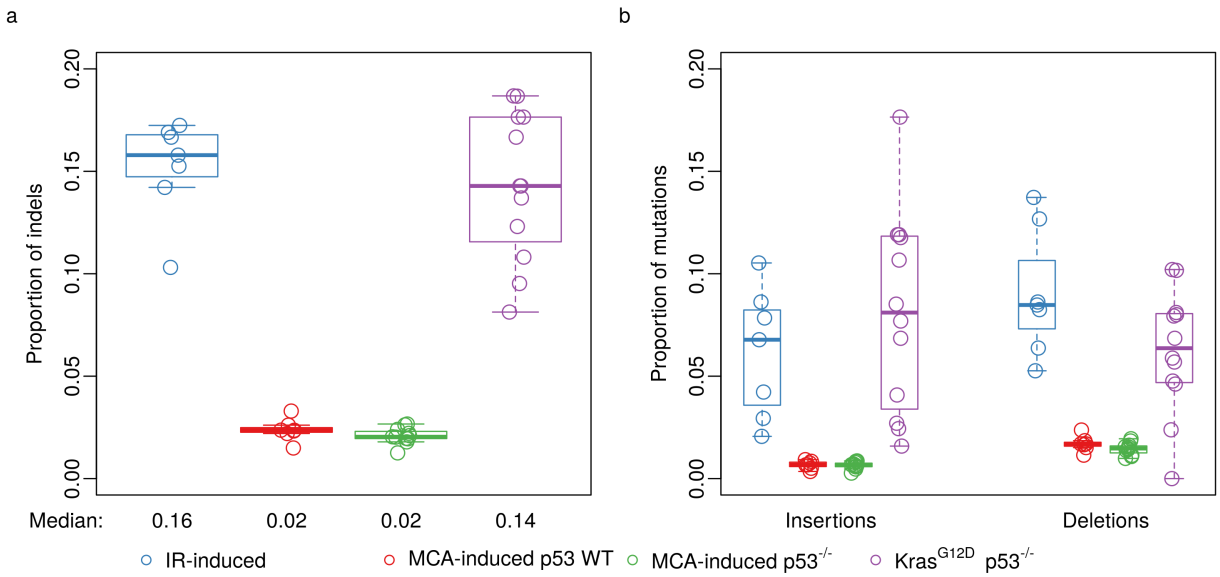

Figure S4. The distribution of sequence variants within total (synonymous and nonsynonymous) somatic mutations. **a,** The proportion of insertion-deletions (indels) within total mutations. **b,** The proportion of insertions or deletions within total mutations.

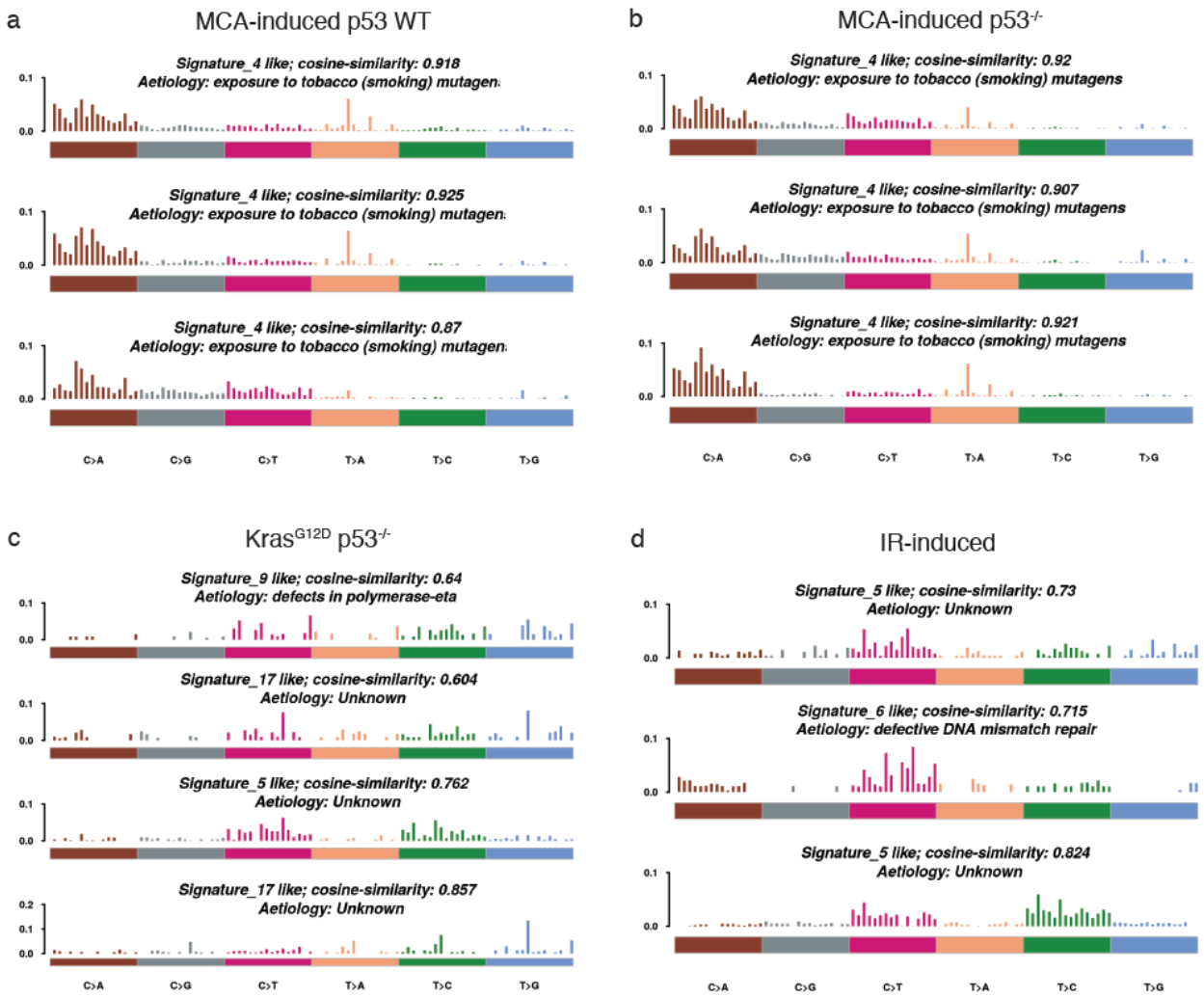

Figure S5. Mutational signature analysis of murine soft-tissue sarcomas. Mutational signatures of each sarcoma genotype were generated using nonnegative matrix factorization (NMF) trinucleotide-based analysis. From each sarcoma genotype, either 3 or 4 individual signatures were generated. Each murine sarcoma signature was compared to COSMIC mutational signatures of human cancers to identify the COSMIC signature with the highest cosine-similarity score.

Figure S6. Schematics of copy number variations across 19 chromosomes of individual sarcoma samples.

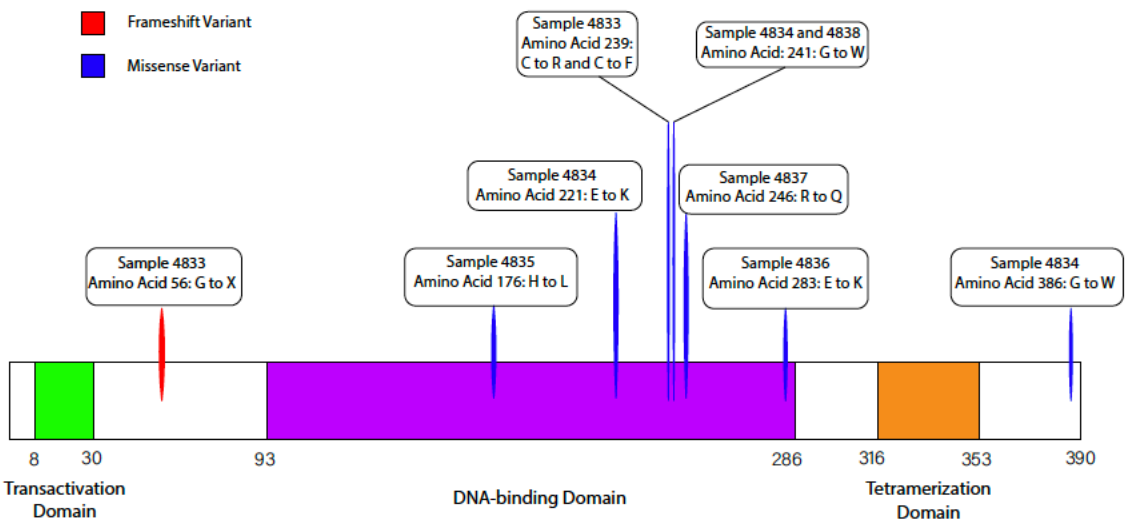

Figure S7. Schematics of nonsynonymous mutations in the tumor suppressor gene p53.

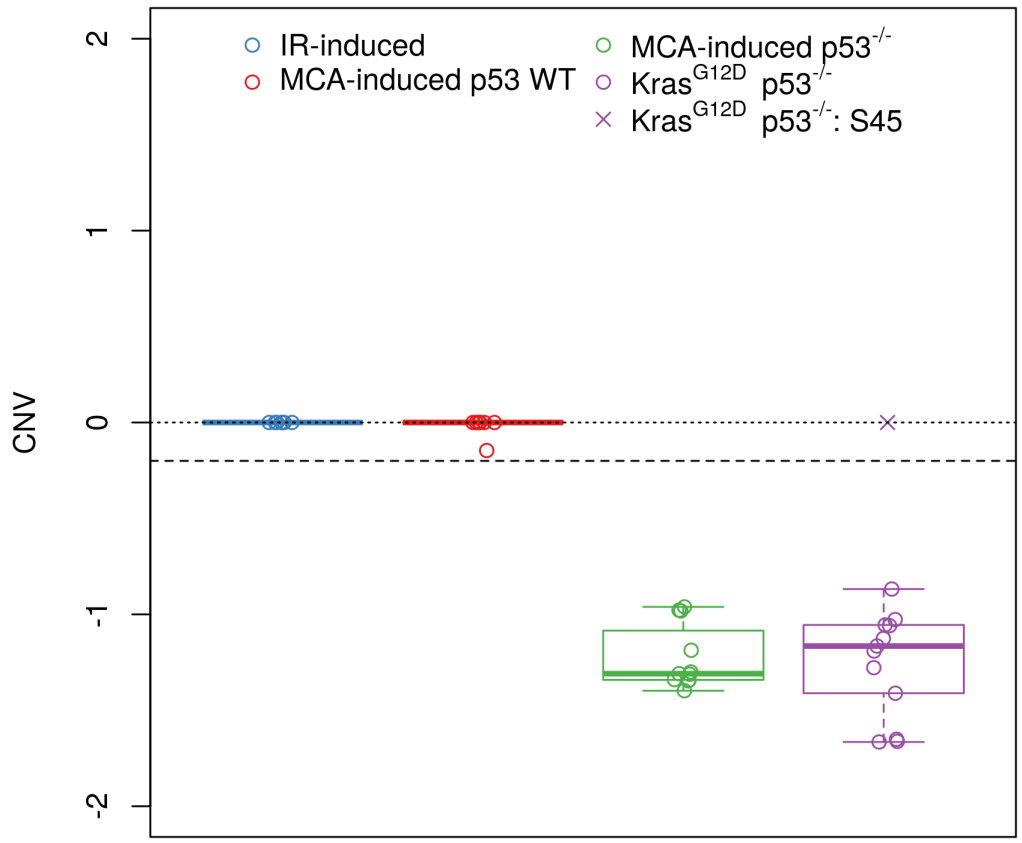

Figure S8. Copy number variations of the tumor suppressor p53 in sarcomas.